Combining Decision Trees with Hierarchical Object-oriented Image Analysis for Mapping Arid Rangelands

Andrea S. Laliberte, Ed L. Fredrickson, and Albert Rango

Abstract

Decision tree analysis is a statistical approach for developing a rule base used for image classification. We developed a unique approach using object-based rather than pixel-based image information as input for a classification tree for mapping arid land vegetation. A QuickBird satellite image was segmented at four different scales, resulting in a hierarchical network of image objects representing the image information in different spatial resolutions. This allowed for differentiation of individual shrubs at a fine scale and delineation of broader vegetation classes at coarser scales. Input variables included spectral, textural and contextual image information, and the variables chosen by the decision tree included many features not available or as easily determined with pixel based image analysis. Spectral information was selected near the top of the classification trees, while contextual and textural variables were more common closer to the terminal nodes of the classification tree. The combination of multi-resolution image segmentation and decision tree analysis facilitated the selection of input variables and helped in determining the appropriate image analysis scale.

Introduction

At the Jornada Experimental Range (JER) operated by the USDA Agricultural Research Service, significant research efforts are focused on multi-scale assessment and monitoring of desert rangelands. Part of this ongoing research program is aimed at determining relationships between ground-based observations and remotely sensed data. The goal of this study was to develop a vegetation classification of a 1,200 ha pasture in order to ascertain the extent and type of grassland and shrub land. Maps derived from this study will serve as inputs for livestock grazing research and techniques applied will help improve vegetation mapping at the JER. Specific objectives of this study were (a) to conduct a multi-scale vegetation analysis of a QuickBird image, and (b) to evaluate an approach of combining object-oriented classification with classification tree analysis (CTA). Grasses were of primary interest for mapping, because they are more palatable to livestock than shrubs. However, the prevalence of honey mesquite shrubs (*Prosopis glandulosa* Torr.) led to an approach of first mapping and masking out shrubs, so that inter-shrub vegetation could be assessed separately. It is hoped that the results of this study will lead to an improved approach for mapping arid land vegetation using high-resolution imagery.

USDA-Agricultural Research Service, Jornada Experimental Range, 2995 Knox St., Las Cruces, NM 88003 (alaliber@nmsu.edu; efredric@nmsu.edu; alrango@nmsu.edu).

Classification of arid land vegetation plant communities often presents unique problems due to the high reflectance of the soil background, a variable mixture of green and senescent grasses, multiple scattering due to open canopies and bright soils, and the prevalence of shrubs in grasslands (Okin and Roberts, 2004), all of which can make it difficult to determine the proportion of grass cover from high-resolution imagery. In addition, when very high spatial resolution imagery (e.g., Ikonos, QuickBird) is used with traditional pixel-based classification, unique problems arise due to a greater degree of shadow and greater spectral variability compared to lower spatial resolution images, all of which can make it difficult to separate classes (Hay *et al.*, 1996). Object-based image analysis offers an alternative, whereby an image segmentation process combines pixels into discrete objects that are homogenous with regard to spatial or spectral characteristics (Ryherd and Woodcock, 1996). Homogeneity in this case refers to smaller within-object than between-object variance.

Object-based segmentation and image classification techniques have been used successfully with very high resolution images of urban areas (Herold *et al.*, 2003; Thomas *et al.*, 2003), for determining shrub encroachment (Hudak and Wessman, 1998, 2001; Laliberte *et al.*, 2004), as well as for various land-use/land-cover mapping projects (Lennartz and Congalton, 2004; van der Sande *et al.*, 2003; Wang *et al.*, 2004). In ecological studies, image segmentation is especially appropriate, because landscapes consist of patches; moreover, due to scale-dependency of objects in a landscape (Turner and Gardner, 1994), segmentation at multiple scales is an approach that offers added insight into ecological processes (Burnett and Blaschke, 2003; Hay *et al.*, 2002).

CTA modeling is a nonparametric statistical technique that helps uncover structure in the data. A dataset is successively split into increasingly homogenous subsets until terminal nodes are determined. In remote sensing, the response variable for a classification tree is a categorical variable (land-use/land-cover class), and for a regression tree the response is a continuous variable (percent cover, percent canopy closure). Explanatory variables can be categorical or continuous (spectral response in bands, elevation, aspect, etc.). The terminal nodes of the tree represent the resulting land-use/land-cover classes; and as such, the tree results in a number of class prediction rules that are used to create a predictive map. CTA has several advantages over linear

Photogrammetric Engineering & Remote Sensing
Vol. 73, No. 2, February 2007, pp. 197–207.

0099-1112/07/7302–0197/$3.00/0

regression models: (a) it is nonparametric and makes no distributional assumptions of any kind, (b) it is not significantly affected by outliers or collinearities, (c) it can detect and reveal variable interactions, (d) both continuous and categorical variables can be used, (e) it handles missing values well, and (f) it is an excellent data reduction tool, capable of finding significant variables if the dataset contains a large number of explanatory variables (Breiman *et al.*, 1984; Clark and Pregibon, 1992).

CTA has been used increasingly in recent years in remote sensing (de Fries *et al.*, 1998; Hansen *et al.*, 1996; Lawrence *et al.*, 2004), and often with better results than other classification approaches. Lawrence and Wright (2001) found that the CTA approach facilitated the use of ancillary data in rule-based classification. Friedl and Brodley (1997) concluded that classification accuracies from decision trees were consistently greater than accuracies obtained using maximum likelihood and linear discriminant function classifiers. Borak and Strahler (1999) determined that the use of a decision tree resulted in a 75 percent reduction in data dimensionality, without significantly degrading classification accuracies.

Object-based classification and CTA complement each other well. The object-based image analysis program eCognition (Baatz and Schaepe, 2000; Definiens, 2003) used in this study outputs hundreds of features that describe image objects created in the segmentation process. Those features include spectral, spatial, textural, and contextual (relationships between neighboring objects and objects at multiple scales) information. The CTA approach is well suited to sort through those numerous features and determine which best describe a terminal class in the classification tree, but a concern for chance agreement does exist.

There are only a few examples in the literature where object-based classification and CTA have been combined in this manner, and in all studies only urban areas were mapped. Thomas *et al.* (2003) used this approach for urban mapping with Airborne Data Acquisition and Registration (ADAR) digital aerial imagery and determined that it increased the accuracy of the map compared to a supervised/unsupervised classification approach, facilitated the determination of features to be used in the classification, and proved to be a time-saving classification approach. Tullis and Jensen (2003) used a decision tree to combine spectral and spatial attributes from image segmentation to detect houses in Ikonos imagery. A similar approach was used by Hodgson *et al.* (2003) for determining imperviousness from aerial photography and lidar (light detection and ranging) data. Those authors found that the combination of decision tree and per-segment classification had the lowest standard error and the highest R^2 value compared to an Isodata and maximum likelihood classification approach.

Our approach is novel in that we are using object-based classification combined with CTA for analyzing arid land vegetation with QuickBird imagery and that we are using multi-resolution segmentation in order to determine the optimal scale for our vegetation analysis.

Methods

Study Site

The Jornada Experimental Range is located approximately 40 km northeast of Las Cruces, New Mexico in the northern part of the Chihuahuan Desert. The area is part of the Jornada del Muerto Basin situated at about 1,200 m elevation between the Rio Grande Valley to the west and the San Andres Mountains to the east. Average monthly maximum temperatures range from 13° C in January to 36° C in June, and mean annual precipitation is 241 mm of which more than 50 percent occurs during July, August, and September. Rainfall amount and distribution is highly variable (Wainwright, inpress). Droughts, defined as years with <75 percent of mean annual precipitation occurred during 18 years between 1915 to 1995 (Havstad *et al.*, 2000). Historically, this area was a semi-desert grassland, but shrub encroachment by honey mesquite has led to a conversion to shrub land. From 1915 to 1998, black grama grass (*Bouteloua eriopoda*) decreased from 19 percent to 1.2 percent, while mesquite increased as a primary dominant from 26 percent to 59 percent (Gibbens *et al.*, 2005). Our study occurred in a 1,200 ha pasture, which represented most of the major vegetation communities at the JER. Dominant grass species included black grama, tobosa (*Pleuraphis mutica*), dropseed (*Sporobolus* spp.), threeawn (*Aristida* spp.), and burrograss (*Scleropogon brevifolius*). Dominant shrub species included honey mesquite, fourwing saltbush (*Atriplex canescens*), soap-tree yucca (*Yucca elata*), Mormon tea (*Ephedra torreyana*), and broom snakeweed (*Gutierrezia sarothrae*). Black grama and tobosa tend to occur in pure stands and are more spectrally distinct than dropseed and threeawn, which are often intermixed, occur with broom snakeweed, and are not easily identified with remote sensing, even in high-resolution imagery. Black grama is more palatable to livestock than the other grass species and therefore of high interest in our mapping effort. Mesquite occurs both as an encroaching shrub to grasslands and as a monoculture in mesquite coppice dunes. In these latter areas, mesquite plants are quite large and easily distinguished because the shrub interspace typically lacks vegetation except during large pulses of rainfall.

Image Data and Preprocessing

A QuickBird satellite image was acquired over the study area on 04 November 2004. The panchromatic (0.61 cm ground resolution) and the multispectral (2.4 m ground resolution) images were pan sharpened using the principal component method in Erdas Imagine® 8.7. Although there are tradeoffs in spectral quality associated with the pan sharpening process (Wald *et al.*, 1997), we chose to use this approach because our objects of interest included both small shrubs to be masked out and only visible in the panchromatic band, as well as vegetation communities that required image analysis with multispectral bands. The preservation of original image radiance values was not as important as the ability to extract small features (shrubs, small vegetation patches, bare areas between shrubs). Moreover, in an object-oriented approach, the radiometric values for individual pixels are averaged for each object, therefore the changes imparted by the pan sharpening process are not as critical as they would be for pixel-based analysis. Pan sharpened imagery has been successfully used in combination with object-oriented analysis for land-cover mapping (van der Sande *et al.*, 2003), determination of land-use intensity (Ivits *et al.*, 2005), and forest classification (Kosaka *et al.*, 2005; Schwarz *et al.*, 2001).

The image was georectified using a second order polynomial function with local ground control points collected from a 1 m resolution digital orthoquad image. Derived image products from the multispectral image included the first principal component (PC1) (which explained 93.53 percent of the total variance) and a soil adjusted vegetation index (SAVI) image. SAVI is designed to minimize the effect of the soil background (Huete, 1988) and is calculated as follows:

$$\text{SAVI} = [(\text{NIR} - \text{red})/(\text{NIR} + \text{red} + \text{L})]*(1 + \text{L}). \quad (1)$$

Similar to an NDVI, the near infrared (NIR) and red bands are used in the calculation, but with the addition of the adjust-

ment factor L. We used an adjustment factor of 0.5, which has been shown to reduce soil influences considerably (Huete, 1988) and is the most widely used adjustment factor for intermediate vegetation cover. Other additional data layers included a soil map, a 10 m DEM, an aspect, and a slope image. Although elevation had a relatively narrow range in the study area (1,313 to 1,338 m), we felt that this feature could help identify certain vegetation classes, such as low lying playa areas that are usually associated with tobosa grass.

Image Segmentation

We used an object-based multiscale image analysis method embedded in the software eCognition (Baatz and Schaepe, 2000; Definiens, 2003). In this approach the image is segmented based on three parameters: scale, color (spectral information), and shape. Color and shape can be weighted from 0 to 1. Within the shape setting, smoothness or compactness can be defined and also weighted from 0 to 1. Scale is a unit-less parameter that controls the size of image objects, with a larger scale parameter resulting in larger image objects. Table 1 shows the segmentation parameters and resulting object statistics for this study. The parameters are determined by visual assessment of the segmentation results and depend on the classification objectives. The segmentation technique in eCognition is a bottom-up region merging technique where smaller image objects are merged into larger ones with the three input parameters controlling the growth in heterogeneity between adjacent image objects. The process stops when the smallest growth exceeds the threshold defined by the scale parameter (Benz *et al.*, 2004). Once segmentation is complete, classification is performed using the segmented objects. To increase the flexibility of the classification, segmentation is usually performed at different scales, which creates a hierarchical network of image objects that represent the image information at different spatial resolutions simultaneously. Image objects can be related contextually, both horizontally at the same segmentation level (neighborhood relations), as well as vertically to the level above (super objects) or below (sub objects).

The workflow of this project is shown diagrammatically in Figure 1. The first step was to mask out all shrubs. Mesquite shrubs occurred throughout the study area, and if shrubs were included in the segmentation, their low spectral values would reduce the overall mean spectral value for an object. By masking the shrubs, we were able to obtain image object attributes that described only shrub interspace vegetation.

In a previous study, we had found that 87 percent of shrubs greater than 2 m^2 could be detected and mapped with the same object-based classification method (Laliberte *et al.*, 2004). We used that same approach to classify shrubs in this study area at the finest segmentation level (level 0). Shrubs were extracted by using the following object features: mean brightness value, mean difference to neighbors, and mean difference to super object (see Table 2 for a definition of features). The resulting classification image

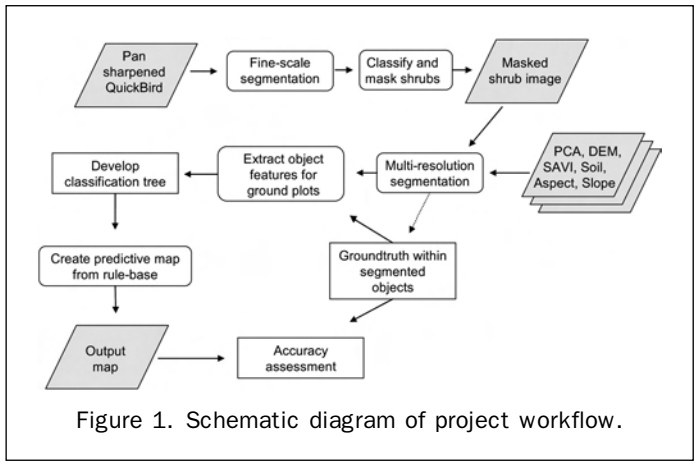

Figure 1. Schematic diagram of project workflow.

was converted into a binary image, setting shrubs to 0 and background to 1. This binary mask was multiplied with the original pan sharpened image to produce a masked shrub image, in which all shrubs had a value of 0. This image was then segmented again at levels 1 to 4. Smaller image objects are nested within the larger ones, and shrubs have been excluded and carry a feature attribute value of 0 (Figure 2).

Ground Sampling

In order to ensure that we would capture the variability in the vegetation, we chose a stratified proportional sampling approach, where the number of plots in each vegetation community was based on the proportional area of that vegetation community. Borak and Strahler (1999) found that proportional sampling resulted in higher accuracy (73.5 percent) than equal sampling (47.2 percent) when using decision trees. In order to delineate vegetation boundaries for the stratified sampling, we created a nearest neighbor classification of the segmented image in eCognition. This requires the user to select sample segments that represent the vegetation type. Those samples were based on visual determination and field visits. The image was classified into four classes: tobosa, dense grass, sparse grass, and other vegetation. This classification was very coarse and only served as a stratification to ensure that the field plots would capture the main vegetation types. After classification, random plots were chosen for each class. We determined that 325 plots should be sufficient for the 1,200 ha area, with each sample plot measuring 2.5 m $\times$ 3.5 m.

At each plot location in the field, we determined the dominant species, estimated percent vegetation cover and took a photo with a digital camera for future reference. The dominant vegetation communities were grouped into four classes: black grama, tobosa, other grasses, and non-grass communities.

TABLE 1. SEGMENTATION PARAMETERS AND RESULTING IMAGE OBJECT STATISTICS

Segmentation Level	Scale Parameter[1]	Color/Shape[2]	Smoothness/Compactness	#of Objects	Mean Area of Objects (sqm)
Level 0	10	0.8/0.2	0.8/0.2	1211433	10
Level 1	100	0.9/0.1	0.5/0.5	10137	1074
Level 2	200	0.9/0.1	0.5/0.5	3256	3288
Level 3	400	0.9/0.1	0.5/0.5	1467	7289
Level 4	600	0.9/0.1	0.5/0.5	1093	9783

[1]Scale parameter is without unit.
[2]Color/shape and smoothness/compactness values are weighting factors ranging from 0 to 1.

TABLE 2. OBJECT FEATURES USED FOR INPUT TO CTA ANALYSIS. THE FEATURES ARE CALCULATED FOR EACH IMAGE OBJECT AND FOR ALL SIX INPUT LAYERS (R, G, B, NIR, PC1, SAVI) EXCEPT WHERE SPECIFIC LAYERS ARE NOTED

Layer Features
Mean of layer: Layer mean value calculated from the values of all pixels forming an image object
Mean DEM: Mean value of elevation calculated from the values of all pixels forming an image object
Aspect: Aspect value of image object
Mean Slope: Mean value of slope calculated from the values of all pixels forming an image object
Soil type: Soil type of image object
Brightness (from R, G, B, NIR): Sum of mean values of R, G, B, NIR for an image object divided by 4
Standard deviation: the standard deviation of the layer values of all pixels forming an image object
Ratio: the layer mean value of an image object divided by the sum of all layer mean values (i.e., ratio (G) = mean (G)/mean (R + G + B + NIR)
Mean difference to neighbors: the mean difference between an image object's mean value and the mean value of all neighboring objects.Individual neighbor differences are weighted by the proportion of boundary they occupy
Mean difference to super object: the mean difference between an image object's mean value and the mean value of its super object
Ratio to super object: the ratio of the mean value of an image object and the mean value of its super object
Standard deviation difference to super object: the difference between the standard deviation of an image object and the standard deviation of its super object
Standard deviation ratio to super object: the ratio of the standard deviation of an image object and the standard deviation of its super object
Mean difference to scene: the difference between the mean value of an image object and the mean value of the whole scene
Ratio to scene: the ratio of the mean value of an image object and the mean value of the whole scene
Texture features
GLCM[1]: the gray level co-occurrence matrix calculated for all pixels of an image object. In order to reduce boundary effects, the pixels bordering the image object are also taken into account. Homogeneity, contrast, dissimilarity, entropy, angular second moment, mean, standard deviation and correlation were calculated.
GLDV[2]: the gray level difference vector calculated for all pixels of an image object. The GLDV is the sum of the diagonals of the GLCM. Angular second moment, entropy, mean, and contrast were calculated
Mean of sub objects: the mean value of the image object's sub object.

[1]Gray level co-occurrence matrix, and [2]gray level difference vector are derived after Haralick et al. (1973). Further detail and formulas for calculating the features can be found in Definiens' eCognition user manual (Definiens, 2003). Definitions for features selected for the level 2 classification tree are found in Table 4.

Extract Object Features for Ground Plots

The next step consisted of extracting the spectral, spatial and contextual features available in eCognition for the segments that contained a plot. It was assumed that field information collected for the plot represented the vegetation for the entire segment. Object features can number in the 100s, because they are calculated for each layer, in this case four spectral bands (R, G, B, NIR) as well as PC1, SAVI, DEM, soil, aspect, and slope. (In this paper, spectral bands will be referred to as *bands*, while derived indices and components will be called *layers*.). Although CTA is non-parametric and correlation between variables is not a great concern, a purely random approach to attribute selection can result in an increase of chance agreement between explanatory and response variables (Lawrence and Wright, 2001), and can produce classification trees that are over fitted and have poor classification accuracy (Liu and White, 1994). For that reason, we excluded some features that would contribute little or nothing to improve the vegetation classification based on a related study (Laliberte *et al.* 2004) and on visual assessment in eCognition's Feature View. The excluded features included mostly shape features, such as area of the segment, width to length ratio, shape index, and border length. Such shape features can be very useful in urban image analysis (Thomas *et al.*, 2003; Tullis and Jensen, 2003), but vegetation cover in our study area is more defined by spectral and contextual features. We did retain features describing spatial relationships between hierarchical levels, because this information was useful in a previous study (Laliberte *et al.*, 2004).

The features that were selected as variables for input to the CTA are divided into layer features and texture features (Table 2). For the DEM layers, we used the mean of the layer for the object. Soil (7 classes) and aspect (N, NE, E, SE, S, SW, W, NW) were used as categorical variables, while for the six remaining input layers (R, G, B, NIR, PC1, SAVI), textural and contextual features were calculated as well. This resulted in a total of 118 object features. Texture features in eCognition are calculated either based on the segment's sub-object, or on the gray level co-occurrence matrix (GLCM) and the gray level difference vector (GLDV) of the object's pixels after Haralick *et al.* (1973). The GLDV is the sum of the diagonals of the GLCM. It counts the number of references to the neighboring pixels' absolute differences (Definiens, 2003), and has shown to be useful in vegetation classifications (Ivits and Koch, 2002).

Classification Tree Analysis

For the decision tree analysis we used CART® by Salford Systems, which uses the algorithm originally developed by Breiman *et al.* (1984). We will use the expression CART® when we refer to the specific program and CTA when referring to classification tree analysis in general. We used half of the sample plots to build the decision tree, and the other half to perform independent accuracy assessments of the resulting predictive maps.

The default splitting rule in CART® is the Gini index (or Gini impurity measure), a measure of heterogeneity. The Gini impurity measure at node t is defined as

$$g(t) = \Sigma p(j)\, p(i) \qquad (2)$$

where p(j) and p(i) are the probability of class j and i at node t. The sum is extended over every class. The Gini index ranges from 0 to 1; it is equal to 0 if all observations in a node belong to the same class, and it is 1 when different class sizes at the node are equal (Breiman *et al.*, 1984; Steinberg and Colla, 1997). In CART®, a maximal tree was grown, and then pruned back to obtain the optimal tree by determining the lowest misclassification errors. The maximal tree is always over-fit, because it represents all idiosyncrasies of the learning data set. The optimal tree was found by ten-fold cross validation. This was done by dividing the learning data set into ten subsamples with an equal distribution for the dependent variable. A maximal tree was grown from 90 percent of the subsamples, with 10 percent of the

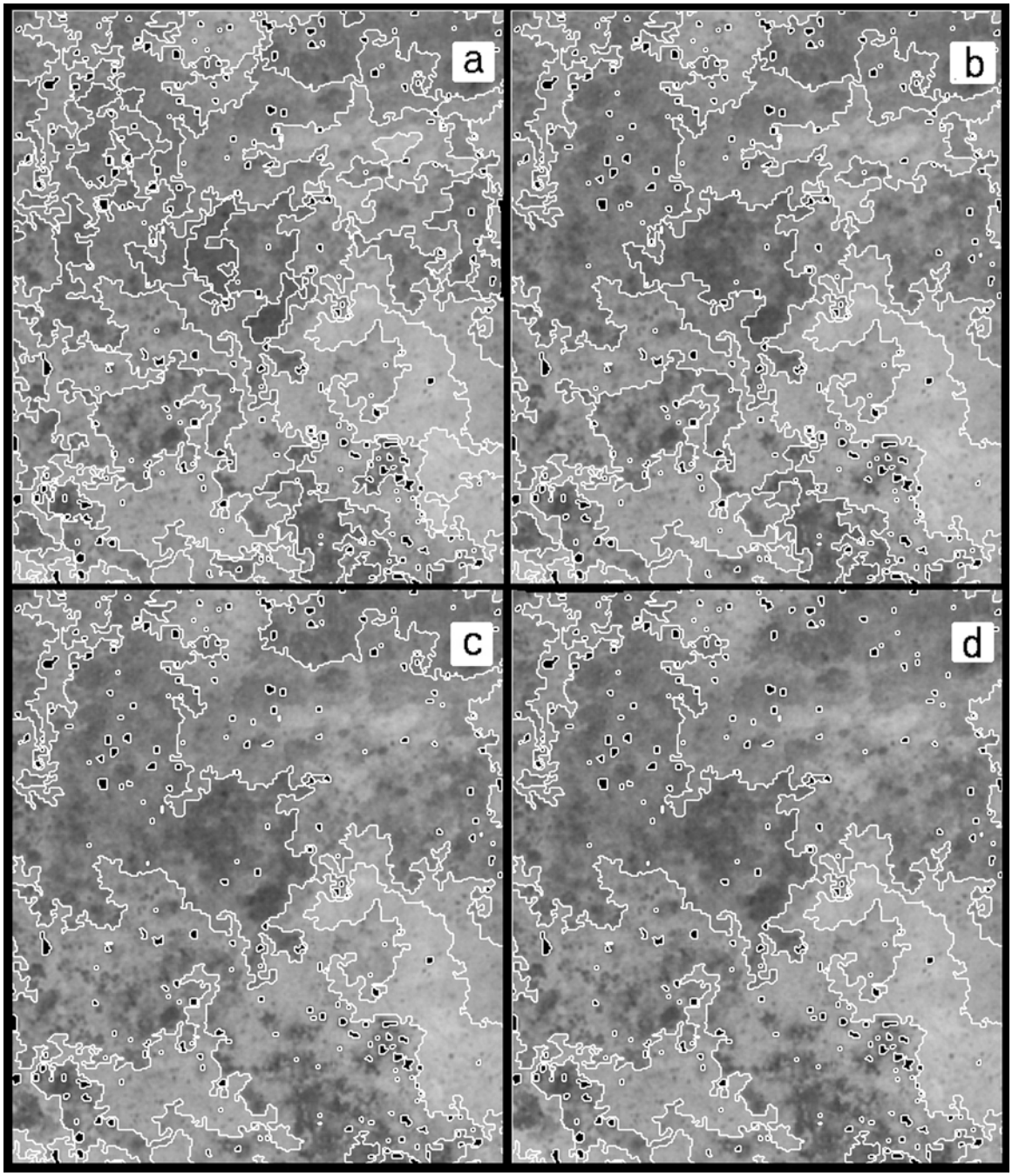

Figure 2. Portion of pan sharpened QuickBird image segmented at level 1 (a), level 2 (b), level 3 (c), level 4 (d). Each image covers an area of 190 m × 223 m. White lines represent image object boundaries. Shrubs excluded from segmentation appear as dark objects.

sample reserved for assessing the misclassification error. This process was repeated ten times with the learning data, each time reserving a different 10 percent of the sample for error assessment. Error rates from the trees were combined to yield estimated error rates for the nodes in the maximal tree. This allowed for determination of error rates for trees of different sizes, and gave an indication of the optimal tree size (Steinberg and Colla, 1997). In addition, to prevent over fitting of the tree, splitting was stopped when a terminal node had less than ten cases. We created decision trees and predictive maps based on each of the four segmentation levels to determine at which level the classification accuracy would be highest. The rule base from CART® was applied in eCognition to create classification maps.

Results

Rule Base and Map Output

The decision tree for level 2 (Figure 3) depicts the rule base used to create the classification for that level. The tree for level 2 is shown here because the map based on those rules

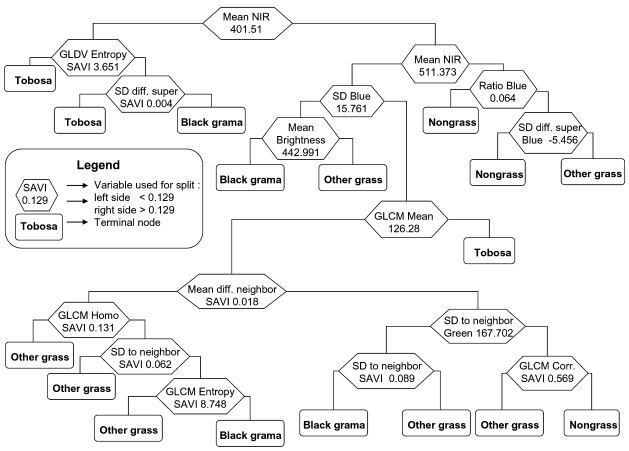

Figure 3. Classification tree for the level 2 segmentation. At each node, a variable and its threshold value is shown in the hexagonal box. Values greater than the one shown in the box are split to the right, values smaller are split to the left. Terminal nodes are shown in bold. For a definition of the variables, see Table 4.

had the highest accuracy at 80 percent (see accuracy assessment below). Both maps (Plate 1) display the same data in a hierarchical fashion. Plate 1b shows the classification with 17 classes, which is one class per terminal node in the classification tree, while in Plate 1a, the 17 classes have been collapsed into the four classes of interest: black grama, tobosa, non-grass, and other grass. This type of display is one of the advantages of using eCognition, which allows the user to group classes together (such as tobosa 1 to 3 into the tobosa group) and switch the view between expanded and collapsed groups. This is advantageous if the rule base requires editing. For example, a black grama terminal node can be changed to nongrass terminal node, and the results can be grouped into a four-class map and visualized immediately. The shrubs that were classified in the finest segmentation and masked out are shown overlaid on the map in black.

Accuracy Assessment

The independent accuracy assessment using the 161 samples showed that overall accuracy was highest at 80 percent for the level 2 segmentation, with very similar results for level 3 at 79 percent overall accuracy (Table 3). The level 2 classification showed higher user's accuracy for black grama and nongrass, while the tobosa and other grass categories showed slightly higher user's accuracy for the level 3

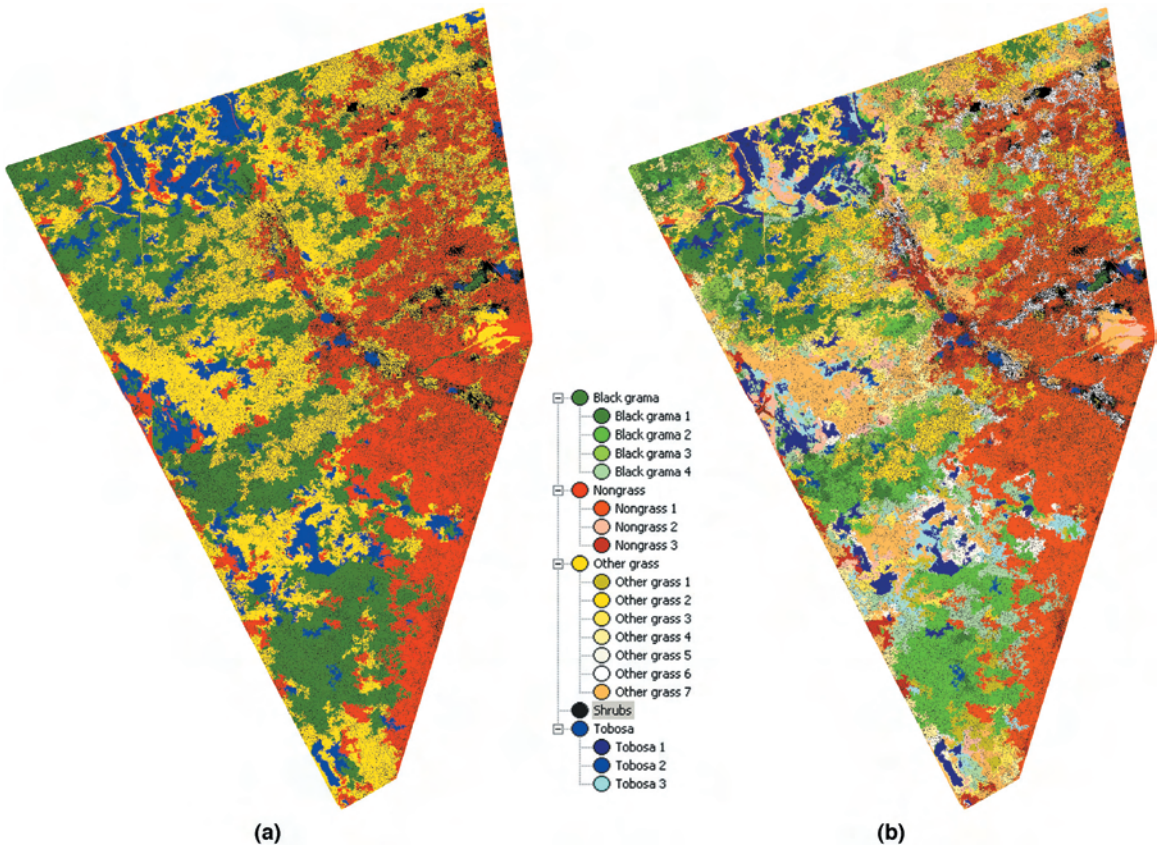

Plate 1. Classification based on classification tree for level 2 segmentation: (a) shows map collapsed into four classes: black grama, tobosa, non-grass, other grass, and (b) shows map expanded into 17 classes, one per terminal node in the classification tree. Shrubs (in black) were derived from a separate classification at the finest segmentation level and were overlaid onto both maps.

TABLE 3. ERROR MATRIX FOR RULE-BASED CLASSIFICATION AT 4 SEGMENTATION LEVELS. ROWS ARE CLASSIFICATION DATA; COLUMNS ARE REFERENCE DATA

Level 1	Black Grama	Other Grasses	Non Grass	Tobosa
Black grama	**28**	12	4	1
Other grasses	7	**22**	5	
Non grass	3	12	**48**	
Tobosa	2	2		**15**
Producer's accuracy	70%	46%	84%	94%
User's accuracy	62%	65%	76%	79%
Overall accuracy	70%			
Kappa index	0.53			

Level 2	Black Grama	Other Grasses	Non Grass	Tobosa
Black grama	**29**	4	1	
Other grasses	8	**37**	7	
Non grass	2	6	**47**	
Tobosa	1	1	2	**16**
Producer's accuracy	73%	77%	82%	100%
User's accuracy	85%	71%	85%	80%
Overall accuracy	80%			
Kappa index	0.72			

Level 3	Black Grama	Other Grasses	Non Grass	Tobosa
Black grama	**32**	4	3	1
Other grasses	5	**35**	8	
Non grass	2	8	**45**	
Tobosa	1	1	1	**15**
Producer's accuracy	80%	73%	79%	94%
User's accuracy	80%	73%	82%	83%
Overall accuracy	79%			
Kappa index	0.71			

Level 4	Black Grama	Other Grasses	Non Grass	Tobosa
Black grama	**34**	10	4	
Other grasses	4	**23**	7	
Non grass	1	10	**44**	
Tobosa	1	5	2	**16**
Producer's accuracy	85%	48%	77%	100%
User's accuracy	71%	68%	80%	67%
Overall accuracy	73%			
Kappa index	0.62			

classification. Due to our interest in the black grama class, the level 2 map was selected as the best map for our use.

The tobosa class showed relatively few misclassification errors in all levels and was represented in all four decision trees by fewer end nodes than the other classes, and those nodes were usually clustered together, all of which indicates lower class variability. The other grass class was confused both with the non-grass class as well as with black grama. The black grama class was well differentiated in levels 2 and 3, but showed confusion with other grasses in levels 1 and 4. A probable reason for this is that a site with mixed grasses can appear spectrally and texturally very similar to a black grama site with lower vegetation cover. Visual inspection of the maps also showed that in levels 1 and 4, higher percent cover black grama areas were consistently classified as black grama, while lower cover black grama was often confused with the other grass class. We assume that at a coarser level segmentation, segments with lower black grama cover and segments of other grass are combined, resulting in greater confusion between black grama and other grasses in level 4. In level 1, it is probable that the segments are small enough that the lower cover black grama sites are separated from those of higher cover and that many are misclassified as other grasses. Levels 2 and 3 appear to segment the image in a way that maximizes the separation of the black grama and other grass class.

Variable Selection in Level 2

In a decision tree approach, the selection of variables and the order in which they appear in the tree are important pieces of information that give insight into relationships between vegetation and remotely sensed variables. In this paper, the terms *object feature* and *variable* are used interchangeably, with object feature relating to the attribute of an image object exported from eCognition and variable describing the same attribute that then becomes an explanatory variable in the CART® analysis. From a total of 118 object features exported from eCognition and used as explanatory variables in CART®, 14 were selected for the level 2 classification tree (Table 4). The variables are classified by category and layer in the table. Category denotes whether a variable is a spectral or textural feature or whether it describes relationships between neighboring, super- or sub-objects. Layer describes the type of input band, index or component that the feature is associated with. Score is an output from the CART® program that reflects the contribution of each variable in classifying or predicting the output class, and scores range from 0 to 100 (Steinberg and Colla, 1997).

The more frequent and earlier in the tree a variable is used, the higher explanatory power it has (Lagacherie and Holmes, 1997), which is reflected in the score. In the level 2 tree, the first variable was the mean of the near-infrared band, and the same variable was used again as a second split. This is not surprising, because the near-infrared band is valuable, often in conjunction with a visible band, for distinguishing vegetation amount. Other variables used in the tree included various measures of texture and relationships to neighboring, super- and sub-objects. The mean of the near-infrared band was the feature with the highest score of 100 due to the fact that it appeared in the first top tiers of the tree and was selected twice. The next highest score was 31.58 for GLDV Entropy SAVI, which was used in the second split of the tree. While a spectral feature had the highest score, textural features appeared 5 times in the tree, neighbor relationships 3 times and super object relationships 2 times. The SAVI was selected 7 times, and it was always selected in conjunction with textural and contextual features in this tree (such as GLCM of SAVI). On the other hand, the near-infrared band was not combined with textural or contextual features, but only selected by its mean spectral value.

While score is a good indicator for the contribution of each variable and for the scale at which it operates, it may be misleading to interpret the score merely as a measure of importance. In our case, the mean of the near-infrared band was the first split, sorting out most of the tobosa classes and the highest cover black grama on one side and the rest of the classes on the other side of the tree. As the tree was split out further, textural and neighbor relation variables were encountered more often. A variable may have a lower score if it appears lower in the tree, but if the terminal node it defines is an important class for the user, then that variable must be considered important as well.

One thing the score can indicate, however, is which variable is most appropriate for a future classification at a comparable segmentation level in a similar vegetation community. If a standard nearest neighbor classification was to be used in eCognition based on selected samples (similar to a supervised classification) (Laliberte *et al.*, 2004), the scores and features chosen for the trees in this study can serve as indicators for feature selection.

TABLE 4. VARIABLE SELECTION AND SCORES FOR THE LEVEL 2 CLASSIFICATION TREE. THE VARIABLES ARE CLASSIFIED BY CATEGORY AND LAYER IN THE TABLE. CATEGORY DENOTES WHETHER A VARIABLE IS A SPECTRAL OR TEXTURAL FEATURE OR WHETHER IT DESCRIBES RELATIONSHIPS BETWEEN NEIGHBORING, SUPER- OR SUB-OBJECTS. LAYER DESCRIBES THE TYPE OF INPUT BAND, INDEX OR COMPONENT THAT THE FEATURE IS ASSOCIATED WITH. SCORE IS AN OUTPUT FROM THE CART® PROGRAM THAT REFLECTS THE CONTRIBUTION OF EACH VARIABLE IN CLASSIFYING OR PREDICTING THE OUTPUT CLASS, AND SCORES RANGE FROM 0 TO 100

Variable (# of times selected)	Definition	Category	Layer	Score
Mean[1] NIR (2)	Mean values of image object in the NIR band	Spectral	NIR	100.00
GLDV[2] Entropy SAVI	Gray level difference vector entropy for SAVI	Texture	SAVI	31.58
StdDev difference to super object SAVI	Difference between the SAVI standard deviation value for an image object and that of its super object	Super object	SAVI	12.82
StdDev Blue	Standard deviation of image object values in the blue band	Spectral	Blue	9.41
StdDev to neighbor SAVI (2)	Difference between the SAVI standard deviation value for an image object and that of its neighbor	Neighbor	SAVI	8.26
Brightness	Mean of the mean values of the red, green, blue, and NIR bands	Spectral	All 4 bands	7.50
Ratio Blue	Mean of the blue band divided by the sum of the mean values of red, green, blue and NIR bands	Spectral	Blue	7.44
GLCM[3] Mean	Gray level co-occurrence matrix mean	Texture	All 4 bands	6.34
Mean difference to neighbor SAVI	Mean difference between the mean value of SAVI and the values of all its neighbor segments	Neighbor	SAVI	6.02
StdDev difference to super object Blue	Difference between the blue band standard deviation value for an image object and that of its super object	Super object	Blue	5.52
StdDev to neighbor green	Difference between the green band standard deviation value for an image object and that of its neighbor	Neighbor	Green	5.41
GLCM Entropy SAVI	Gray level co-occurrence matrix entropy for SAVI	Texture	SAVI	4.61
GLCM Correlation SAVI	Gray level co-occurrence matrix correlation for SAVI	Texture	SAVI	4.26
GLCM Homogeneity SAVI	Gray level co-occurrence matrix homogeneity for SAVI	Texture	SAVI	4.06

[1]Calculations for statistics are derived using all pixels forming an image object.
[2]Gray level difference vector and [3]Gray level co-occurrence matrix are derived after Haralick et al. (1973). Further detail and formulas for calculating the features can be found in Definiens' eCognition user manual (Definiens, 2003).

Variable Selection in All Segmentation Levels

Although the accuracy at levels 1, 3, and 4 was lower than level 2, we were still interested in comparing variable selection and scores for all 4 levels, because this information can give insight about at which segmentation scale a variable is selected, and whether the variable operates near the top or the bottom of the tree within a segmentation level. We grouped each variable in two ways: (a) by category (texture, spectral, neighbor relationship, super-/sub-object relationship, soil and DEM), and (b) by layer (near-infrared, red, green, blue, all four bands, SAVI, PC1) and sorted the information first by segmentation level, then by score.

The category grouping (Table 5) indicates that texture, spectral and neighbor information was selected in all segmentation levels, but the lower scores of texture mean that textural features appeared closer to the terminal nodes in the decision tree. In all four classification trees, the first variable in the tree was either the mean of the near-infrared or the mean difference to the neighbor, and textural features were found lower in the classification tree. The highest scores were found with spectral information in levels 1 and 2 and neighbor relationships in levels 3 and 4. Neighbor relationships played a bigger role in the coarser segmentation, because in our segmentation scheme, the difference to a neighboring object was larger in the coarser than the finer segmentation. This might not be the case in other segmentation hierarchies, because the changes in differences to neighboring objects depend on the relative scale parameter used as well as the relative differences between the scale parameters for each level.

Variables relating to super- and sub-objects were used in all levels except level 3, and those variables appeared lower in the tree similar to texture. The soil variable was not used in levels 2 and 3, but appeared as the second split variable in the level 1 decision tree. We expected that soil would be a useful variable at any scale, and are unsure why it was not selected for all levels. The elevation variable was only used at the coarser segmentation levels, which makes sense, because we used a 10 m resolution DEM. At level 4, elevation appeared as the third split variable in the tree, and as expected it separated tobosa in the lower lying playa areas from the other vegetation classes.

Although not shown here, among the eight GLCM features (angular second moment, contrast, correlation, entropy, dissimilarity, homogeneity, mean, and standard deviation) and the four GLDV features (angular second moment, contrast, entropy, and mean) available in eCognition, entropy was selected most often (5 times and 2 times in combination with SAVI). Entropy measures the degree of disorder or heterogeneity in an image, and this particular texture measurement has been found useful in mapping vegetation (Franklin *et al.*, 2000).

TABLE 5. VARIABLES USED IN THE CLASSIFICATION TREES SORTED BY CATEGORY (TEXTURE, SPECTRAL, NEIGHBOR, ETC.), SEGMENTATION LEVEL (1 TO 4), AND SCORE DERIVED FROM THE CART® PROGRAM

Texture		Spectral		Neighbor		Super/Subobject		Soil		DEM	
Level	Score	Level	Score	Level	Score	Level	Score	Level	Score	Level	Score
1	10.63	1	100.00	1	15.70	1	7.58	1	31.55	3	13.25
1	5.89	1	16.11	2	8.26	2	12.82	4	10.06	4	16.04
1	5.23	1	11.26	2	6.02	2	5.52				
1	3.53	2	100.00	2	5.41	4	7.41				
1	2.95	2	9.41	3	100.00	4	1.91				
2	31.58	2	7.50	3	7.09						
2	6.34	2	7.44	4	100.00						
2	4.61	3	64.43	4	12.21						
2	4.26	3	30.17	4	7.90						
2	4.06	3	27.63	4	7.67						
3	17.30	3	25.76	4	5.41						
3	9.24	3	13.16	4	3.25						
3	8.36	3	12.85	4	1.66						
3	7.11	3	7.93								
3	6.07	4	54.41								
3	5.92	4	7.30								
4	14.34	4	5.53								
4	9.61										

The layer grouping (Table 6) showed the highest scores for NIR (levels 1 and 2), PC1 (level 3), and red band (level 4). Overall, the near-infrared band had the highest scores, meaning it was selected early in the tree. The green and blue bands as well as SAVI were found more frequently in the lower part of the decision tree, and SAVI was the most frequently selected variable. SAVI, the blue and NIR bands were selected in all four levels, while the red band was not found in the level 1 and 2 decision trees. The blue band was selected more frequently than the red or green band; most of those selections (5 of 9) were relationships to neighbor and super objects. The blue band is generally noisier and more affected by atmospheric scattering than other bands, but in spite of this was useful in our study.

Discussion and Conclusions

The hierarchical segmentation approach used in this study was well suited for distinguishing features at different scales. Shrubs were segmented and classified at a fine scale and masked out, so that shrub-interspace vegetation could be analyzed at coarser scales. We chose four segmentation levels to determine the scale that yielded the highest classification accuracy. A decision tree approach was chosen, because eCognition creates hundreds of spectral, spatial, textural, and contextual object features. Although a feature space optimization is available in eCognition (Definiens, 2003), it relies on object training samples and nearest neighbor classification, whereas we were interested in the use of decision trees and rule based classification for this study. In addition, the feature space optimization only defines features to use, not a rule base for the features.

The approach of combining object-based image analysis with decision trees was an excellent data reduction tool for the numerous object features. The strength of the decision tree lay in selecting useful features from a large number of possible features. Correlation between features was not a great concern, because decision trees are non-parametric, nonetheless, we excluded features that we knew would not contribute to the analysis. The application of the rule base in eCognition, the classification and class display were straightforward. Moving back and forth between collapsing and expanding classes based on either all nodes of the classification tree or the final classification scheme was an especially useful feature for visualizing misclassifications.

Aside from incorporating textural information, traditional pixel-based classification has mostly relied on spectral information. With the advent of high-resolution satellite

TABLE 6. VARIABLES USED IN THE CLASSIFICATION TREES SORTED BY LAYER, SEGMENTATION LEVEL AND SCORE DERIVED FROM THE CART® PROGRAM

SAVI		All 4 Bands		Blue		PC1		NIR		Red		Green	
Level	Score	Level	Score	Level	Score	Level	Score	Level	Score	Level	Score	Level	Score
1	2.95	1	16.11	1	15.70	1	5.89	1	100.00	3	27.63	2	5.41
2	31.58	1	10.63	1	11.26	3	100.00	2	100.00	3	7.09	3	7.93
2	12.82	1	5.23	2	9.41	3	8.36	3	63.43	4	100.00	4	7.41
2	8.26	1	3.53	2	7.44	3	5.92	3	13.16	4	7.90	4	7.30
2	6.02	2	7.50	2	5.52	4	54.41	4	5.53	4	7.67		
2	4.61	2	6.34	3	12.85	4	14.34	4	1.66	4	1.91		
2	4.26	3	25.76	4	12.21	4	9.61						
2	4.06	3	17.30	4	5.14								
3	30.17	3	7.11	4	3.25								
3	9.24												
3	6.07												

imagery, techniques traditionally used with manual aerial photo interpretation are now finding their way into automated image analysis. Features such as shape, size, pattern, tone, texture, shadows, site, and association are characteristics more commonly associated with aerial photo interpretation (Lillesand and Kiefer, 2000), but have been found to be increasingly useful with very high-resolution satellite imagery and digital aerial photography (van der Sande *et al.*, 2003; Wulder *et al.*, 1998).

The variables selected by CART® in our study included many features that are not as easily determined or incorporated in traditional pixel based image analysis, but are routinely calculated in eCognition. Spectral information was selected most often at or near the top of the classification trees, while contextual and textural variables were selected near the terminal nodes of the classification tree. This was observed in all four segmentation levels and indicates that more subtle distinctions are made in the statistical data using textural and contextual information. Differences in the variable selection between segmentation levels related mostly to the fact that in a coarser segmentation, differences to neighbors were more pronounced, and therefore, variables describing relationships to neighbors were selected more often and had a higher score in levels 3 and 4 than in levels 1 and 2.

In the level 2 tree, the highest cover tobosa and black grama classes were sorted out in the first split in the tree by the mean of the near infrared band. A second split with the mean of the near-infrared separated the lowest vegetation cover and bare areas from the remaining classes. This makes ecological sense, because the most spectrally distinct classes (tobosa and dense black grama) were defined first. Less spectrally distinct classes, such as mixed grasses and lower cover black grama, were sorted out lower in the tree, mostly by variables incorporating SAVI and textural features. The SAVI was the most frequently selected layer, and was always used in conjunction with textural or contextual features. We did not incorporate other vegetation indices, because in general, most vegetation indices are insensitive to non photosynthetic vegetation, but sensitive to soil color (Okin and Roberts, 2004). However, our results appear to indicate that second order statistics derived from SAVI were useful features for vegetation classification in our study.

Texture variables based on the gray level co-occurrence matrix appeared in the lower part of the classification tree, indicating that they are useful for subtle discriminations in communities with mixed grasses and low to intermediate vegetation cover. Textural information based on second order statistics has been shown to improve classification accuracy over using only spectral information (Moskal and Franklin, 2002; Tuominen and Pekkarinen, 2004), and Franklin *et al.* (2000) found that the addition of texture improved higher resolution images more than lower resolution images. Contextual variables describing relationships between neighboring objects or between super- and sub-objects were found in all decision trees and had overall a relatively high score, especially in the coarser segmentation levels.

The classification accuracy of 80 percent for the level 2 decision tree was satisfactory for arid vegetation mapping considering that we were able to separate black grama and tobosa from other grass species and non-grass areas. Although we broke down two of our classes (other grass and non-grass) further in the field, the resulting sample size in some of those classes was relatively small. Because CTA is sensitive to large differences in sample sizes among classes, we were not able to construct decision trees with half the samples and estimate accuracy with the other half for a larger number of classes.

In a future study, we intend to compare our results with those of a nearest neighbor classification approach with training samples. Using larger training areas on the ground might be more appropriate in conjunction with an object-based analysis, because ground training sites and image objects will be of similar size. This approach will also allow for comparing a feature space optimization method with the decision tree method.

This study shows that the combination of multi-resolution segmentation and classification tree analysis can be an effective method for mapping arid rangeland vegetation at the pasture-level scale. It allows for incorporating ancillary data layers, facilitates the evaluation of numerous spectral, textural, and contextual features of the input layers, and helps in determining the appropriate analysis scale. Future related research will concentrate on applying this technique over larger areas and with medium-resolution satellite imagery such as ASTER or Landsat.

Acknowledgments

This research was funded by the USDA Agricultural Research Service and the National Science Foundation Long-Term Ecological Research Program, Jornada Basin IV: Linkages in Semiarid Landscapes

References

Baatz, M., and A. Schaepe, 2000. Multiresolution segmentation: An optimization approach for high quality multi-scale image segmentation, *Angewandte Geographische Informationsverarbeitung* (J. Strobl and T. Blaschke, editors), Vol.XII, Wichmann, Heidelberg, Germany, pp. 12–23.

Benz, U.C., P. Hoffmann, G. Willhauck, I. Lingenfelder, and M. Heynen, 2004. Multi-resolution, object-oriented fuzzy analysis of remote sensing data for GIS-ready information, *ISPRS Journal of Photogrammetry and Remote Sensing*, 58:239–258.

Borak, J.S., and A.H. Strahler, 1999. Feature selection and land cover classification of a MODIS-like data set for a semiarid environment, *International Journal of Remote Sensing*, 20(5): 919–938.

Breiman, L., J.H. Friedman, R.A. Olshen, and C.J. Stone, 1984. *Classification and Regression Trees*, Wadsworth International Group, Belmont, California, 358 p.

Burnett, C., and T. Blaschke, 2003. A multi-scale segmentation/object relationship modelling methodology for landscape analysis, *Ecological Modelling*, 168(3):233–249.

Clark, L.A., and D. Pregibon, 1992. Tree-based models, *Statistical Models in S* (J.M. Chambers and T.J. Hastie, editors), Wadsworth & Brooks/Cole Advanced Books & Software, Pacific Grove, California, pp. 377–419.

de Fries, R.S., J.R.G. Townshend, M. Hansen, and R. Sohlberg, 1998. Global land cover classifications at 8 m spatial resolution: The use of training data derived from Landsat imagery in decision tree classifiers, *International Journal of Remote Sensing*, 19(16): 3141–3168.

Definiens, 2003. eCognition User Guide, Version 4.0, URL: *http://www.definiens-imaging.com*. (last date accessed: 15 November 2006).

Franklin, S.E., R.J. Hall, L.M. Moskal, A.J. Maudie, and M.B. Lavigne, 2000. Incorporating texture into classification of forest species composition from airborne multispectral images, *International Journal of Remote Sensing*, 21(1): 61–79.

Friedl, M.A., and C.E. Brodley, 1997. Decision tree classification of land cover from remotely sensed data, *Remote Sensing of Environment*, 61:399–409.

Gibbens, R.P., R.P. McNeely, K.M. Havstad, R.F. Beck, and B. Nolen, 2005. Vegetation changes in the Jornada Basin from 1858 to 1998, *Journal of Arid Environments*, 61:651–668.

Hansen, M., R. Dubayah, and R. de Fries, 1996. Classification trees: An alternative to traditional land cover classifiers, *International Journal of Remote Sensing*, 17(5):1075–1081.

Haralick, R., K. Shanmugan, and I. Dinstein, 1973. Textural features for image classification, *IEEE Transactions on Systems, Man and Cybernetics*, 3(1):610–621.

Havstad, K.M., W.P. Kustas, A. Rango, J.C. Ritchie, and T.J. Schmugge, 2000. Jornada experimental range: A unique arid land location for experiments to validate satellite systems, *Remote Sensing of Environment*, 74:13–25.

Hay, G.J., K.O. Niemann, and G.F. McLean, 1996. An object-specific image-texture analysis of H-resolution forest imagery, *Remote Sensing of Environment*, 55:108–122.

Hay, G.J., P. Dube, A. Bouchard, and D.J. Marceau, 2002. A scale-space primer for exploring and quantifying complex landscapes, *Ecological Modelling*, 153:27–49.

Herold, M, X. Liu, and K.C. Clarke, 2003. Spatial metrics and image texture for mapping urban land use, *Photogrammetric Engineering & Remote Sensing*, 69(9):991–1001.

Hodgson, M.E., J.R. Jensen, J.A. Tullis, K.D. Riordan, and C.M. Archer, 2003. Synergistic use of lidar and color aerial photography for mapping urban parcel imperviousness, *Photogrammetric Engineering & Remote Sensing*, 69(9):973–980.

Hudak, A.T., and C.A. Wessman, 1998. Textural analysis of historical aerial photography to characterize woody plant encroachment in South African savanna, *Remote Sensing of Environment*, 66:317–330.

Hudak, A.T., and C.A. Wessman, 2001. Textural analysis of high resolution imagery to quantify bush encroachment in Makidwe Game Reserve, South Africa, 1955–1996, *International Journal of Remote Sensing*, 22(14):2731–2740.

Huete, A.R., 1988. A soil-adjusted vegetation index (SAVI), *Remote Sensing of Environment*, 25:295–309.

Ivits, E., B. Koch, T. Blaschke, M. Jochum, and P. Adler, 2005. Landscape structure assessment with image grey-values and object-based classification, *International Journal of Remote Sensing*, 26(14):2975–2993.

Ivits, E., and B. Koch, 2002. Object-oriented remote sensing tools for biodiversity assessment: A European approach, *Proceedings of the 22nd EARSeL Symposium*, 04–06 June, Prague, Czech Republic, Millpress Science Publishers, Rotterdam, Netherlands, unpaginated CD-ROM.

Kosaka, N., T. Akiyama, B. Tsai, and T. Kojima, 2005. Forest type classification using data fusion of multispectral and panchromatic high-resolution satellite imagery, *Proceedings of the 2005 Geoscience and Remote Sensing Symposium, IGARSS '05*, 25–29 July, Seoul, Korea, IEEE International, unpaginated CD-ROM.

Lagacherie, P., and S. Holmes, 1997. Addressing geographical data errors in a classification tree for soil unit prediction, *International Journal of Geographical Information Science*, 11(2):183–198.

Laliberte, A.S., A. Rango, K.M. Havstad, J.F. Paris, R.F. Beck, R. McNeely, and A.L Gonzalez, 2004. Object-oriented image analysis for mapping shrub encroachment from 1937–2003 in southern New Mexico, *Remote Sensing of Environment*, 93:198–210.

Lawrence, R.L., A. Bunn, S. Powell, and M. Zambon, 2004. Classification of remotely sensed imagery using stochastic gradient boosting as a refinement of classification tree analysis, *Remote Sensing of Environment*, 90:331–336.

Lawrence, R.L., and A. Wright, 2001. Rule-based classification systems using classification and regression trees (CART) analysis, *Photogrammetric Engineering & Remote Sensing*, 67(10):1137–1142.

Lennartz, S.P., and R.G. Congalton, 2004. Classifying and mapping forest cover types using Ikonos imagery in the northeastern United States, *Proceedings of the ASPRS Annual Conference*, 24–28 May, Denver, Colorado, American Society for Photogrammetry and Remote Sensing, Bethesda, Maryland, unpaginated CD-ROM.

Lillesand, T.M., and R.W. Kiefer, 2000. *Remote Sensing and Image Interpretation*, 4th Edition, John Wiley and Sons, Inc., New York, 724 p.

Liu, W.Z., and A.P. White, 1994. The importance of attribute selection measures in decision tree induction, *Machine Learning*, 15:25–41.

Moskal, L.M., and S.E. Franklin, 2002. Multi-layer forest stand discrimination with spatial co-occurrence texture analysis of high spatial detail airborne imagery, *Geocarto International*, 17(4):53–65.

Okin, G.S., and D.A. Roberts, 2004. Remote Sensing in Arid Regions: Challenges and Opportunities, *Manual of Remote Sensing, Volume 4, Remote Sensing for Natural Resource Management and Environmental Monitoring* (S.L. Ustin, editor), John Wiley and Sons, Inc., New York, pp. 111–146.

Ryherd, S., and C. Woodcock, 1996. Combining spectral and texture data in the segmentation of remotely sensed images, *Photogrammetric Engineering & Remote Sensing*, 62(2):181–194.

Schwarz, M., C. Steinmeier, and L. Waser, 2001. Detection of storm losses in alpine forest areas by different methodic approaches using high-resolution satellite data, *Proceedings of the 21st EARSeL Symposium: Observing our Environment from Space: New Solutions for a New Millenium*, 14–16 May, Paris, France, A.A. Balkema, Leiden, Netherlands, pp. 251–257.

Steinberg, D., and P. Colla, 1997. *CART – Classification and Regression Trees: Supplementary Manual for Windows*, Salford Systems, San Diego, California.

Thomas, N., C. Hendrix, and R.G. Congalton, 2003. A comparison of urban mapping methods using high-resolution digital imagery, *Photogrammetric Engineering & Remote Sensing*, 69(9):963–972.

Tullis, J.A., and J.R. Jensen, 2003. Expert system house detection in high spatial resolution imagery using size, shaper, and context, *Geocarto International*, 18(1):5–15.

Tuominen, S., and A. Pekkarinen, 2004. Performance of different spectral and textural aerial photograph features in multi-source forest inventory, *Remote Sensing of Environment*, 94:256–268.

Turner, M.G., and R.H. Gardner, 1994. *Quantitative Methods in Landscape Ecology*, Springer-Verlag, New York, New York, 536 p.

van der Sande, C.J., S.M. de Jong, and A.P.J. de Roo, 2003. A segmentation and classification approach of IKONOS-2 imagery for land cover mapping to assist flood risk and flood damage assessment, *International Journal of Applied Earth Observation and Geoinformation*, 4:217–229.

Wainwright, J., 2006. Climate and climatological variations in the Jornada Basin, *Structure and Function of a Chihuahuan Desert Ecosystem: The Jornada Basin Long-term Ecological Research Site* (K.M. Havstad, L. Huenneke, and W.H. Schlesinger, editors), Oxford University Press, New York, New York, 492 p.

Wald, L., T. Ranchin, and M. Mangolini, 1997. Fusion of satellite images of different spatial resolution: Assessing the quality of resulting images, *Photogrammetric Engineering & Remote Sensing*, 63(6):691–699.

Wang, L., W.P. Sousa, and P. Gong, 2004. Integration of object-based and pixel-based classification for mapping mangroves with IKONOS imagery, *International Journal of Remote Sensing*, 25(24):5655–5668.

Wulder, M.A., E.F. LeDrew, S.E. Franklin, and M.B. Lavigne, 1998. Aerial image texture information in the estimation of northern deciduous and mixed wood forest leaf area index (LAI), *Remote Sensing of Environment*, 64:64–76.

(Received 11 May 2005; accepted 05 October 2005; revised 07 November 2005)